Inorg. Chem. **2002**, *41*, 3259–3268

Investigation of Silver Salt Metathesis: Preparation of Cationic Germanium(II) and Tin(II) Complexes, and Silver Adducts Containing Unsupported Silver–Germanium and Silver–Tin Bonds

Ashley E. Ayers and H. V. Rasika Dias*

Department of Chemistry and Biochemistry, Box 19065, The University of Texas at Arlington, Arlington, Texas 76019-0065

Received January 25, 2002

Syntheses of halide derivatives of germanium(II) and tin(II) aminotroponiminate (ATI) complexes and their silver salt metathesis reactions have been investigated. The treatment of $GeCl_2$•(1,4-dioxane), $SnCl_2$, or SnI_2 with [(*n*-Pr)$_2$ATI]Li in a 1:1 molar ratio affords the corresponding germanium(II) or tin(II) halide complex [(*n*-Pr)$_2$ATI]MX (where [(*n*-Pr)$_2$ATI]$^-$ = *N*-(*n*-propyl)-2-(*n*-propylamino)troponiminate; M = Ge or Sn; X = Cl or I). As usually expected, [(*n*-Pr)$_2$ATI]GeCl and [(*n*-Pr)$_2$ATI]SnCl undergo rapid metathesis with CF_3SO_3Ag, leading to trifluoromethanesulfonate salts, {[(*n*-Pr)$_2$ATI]Ge}[SO_3CF_3] and {[(*n*-Pr)$_2$ATI]Sn}[SO_3CF_3], and silver chloride. However, when the silver source [HB(3,5-$(CF_3)_2$Pz)$_3$]Ag(η^2-toluene) is used, rather than undergoing metathesis, very stable 1:1 adducts [HB(3,5-$(CF_3)_2$Pz)$_3$]Ag←Ge(Cl)[(*n*-Pr)$_2$ATI] and [HB(3,5-$(CF_3)_2$Pz)$_3$]Ag←Sn(Cl)[(*n*-Pr)$_2$ATI] are formed (where [HB(3,5-$(CF_3)_2$Pz)$_3$]$^-$ = hydrotris(3,5-bis(trifluoromethyl)pyrazolyl)borate). The use of the iodide derivative [(*n*-Pr)$_2$ATI]SnI did not change the outcome either. All new compounds have been characterized by multinuclear NMR spectroscopy and X-ray crystallography. The Ag–Ge and Ag–Sn bond distances of [HB(3,5-$(CF_3)_2$Pz)$_3$]Ag←Ge(Cl)[(*n*-Pr)$_2$ATI], [HB(3,5-$(CF_3)_2$Pz)$_3$]Ag←Sn(Cl)[(*n*-Pr)$_2$ATI], and [HB(3,5-$(CF_3)_2$Pz)$_3$]Ag←Sn(I)[(*n*-Pr)$_2$ATI] are 2.4142(6), 2.5863(6), and 2.5880(10) Å, respectively. A convenient route to [(*n*-Pr)$_2$ATI]H is also reported.

Introduction

For most metal halides (LMX) and silver derivatives (AgY), silver salt metathesis reactions proceed quite rapidly and smoothly.[1] The reaction is driven toward product formation by silver halide precipitation and is the preferred method for introducing weakly coordinating anions to a metal center.[1−3]

$$\mathrm{LMX} + \mathrm{AgY} \xrightarrow[\mathrm{X^-} = \text{halide ion}]{} \mathrm{LMY} + \mathrm{AgX}$$

Even though silver salt metathesis reactions occur for many different metal halides and silver compounds, there are cases in which silver halide precipitation is either very slow or inhibited.[2−9] In rare cases, stable isolable products may be obtained from these reactions. For example, metathesis between $CpFe(CO)_2I$ and $Ag(B_{11}CH_{12})$ takes about one week to go to completion.[1] It is possible to isolate a stable intermediate $CpFe(CO)_2I{\rightarrow}Ag(B_{11}CH_{12})$ from this mixture and characterize it using spectroscopic methods. When the counterion is BF_4^-, the iodide bridged intermediate can be observed in solution but decomposes more rapidly to generate AgI and $CpFe(CO)_2(BF_4)$.[7] The reaction between $CpMo(CO)_3I$ and $Ag(B_{11}CH_{12})$ is also slow. This mixture affords an isolable intermediate $[CpMo(CO)_3Ir{\rightarrow}Ag(CB_{11}H_{12})]_2$, which is dimeric in the solid state.[5,6] Other types of intermediates with different types of linkages have also been reported. For example, when $(PPh_3)_2(CO)IrCl$ is treated with

* Author to whom correspondence should be addressed. E-mail: dias@uta.edu.

(1) Liston, D. J.; Lee, Y. J.; Scheidt, W. R.; Reed, C. A. *J. Am. Chem. Soc.* **1989**, *111*, 6643−6648.
(2) Strauss, S. H. *Chem. Rev.* **1993**, *93*, 927−942.
(3) Reed, C. A. *Acc. Chem. Res.* **1998**, *31*, 133−139.
(4) Xie, Z.; Jelinek, T.; Bau, R.; Reed, C. A. *J. Am. Chem. Soc.* **1994**, *116*, 1907−1913.
(5) Patmore, N. J.; Weller, A. S.; Steed, J. W. *Chem. Commun.* **2000**, 1055−1056.
(6) Patmore, N. J.; Mahon, M. F.; Steed, J. W.; Weller, A. S. *J. Chem. Soc., Dalton Trans.* **2001**, 277−283.
(7) Mattson, B. M.; Graham, W. A. G. *Inorg. Chem.* **1981**, *20*, 3186−3189.
(8) Dias, H. V. R.; Wang, Z. *Inorg. Chem.* **2000**, *39*, 3890−3893.
(9) McNeil, W. S.; DuMez, D. D.; Matano, Y.; Lovell, S.; Mayer, J. M. *Organometallics* **1999**, *18*, 3715−3727. Bellachioma, G.; Cardaci, G.; Macchioni, A.; Valentini, F.; Zuccaccia, C.; Foresti, E.; Sabatino, P. *Organometallics* **2000**, *19*, 4320−4326.

10.1021/ic0200747 CCC: $22.00 © 2002 American Chemical Society
Published on Web 05/18/2002

$Ag(B_{11}CH_{12})$[1,10] or $Ag(Br_5CB_9H_5)$,[4] no precipitation of AgCl is observed even after several days. Instead, thermally stable adducts such as $(PPh_3)_2(CO)(Cl)Ir\rightarrow Ag(B_{11}CH_{12})$ that feature Ir−Ag bonds are formed. The chloride ion of the iridium adduct $(PPh_3)_2(CO)IrCl$ can however be readily abstracted using $AgClO_4$. The study of these species and related models of likely intermediates are important because they offer important insight into the mechanism of silver salt metathesis, a process not well understood for inorganic systems.

An area of research focus in this laboratory is the chemistry of *N*-alkyl-2-(alkylamino)troponiminate ($[(R)_2ATI]^-$) derivatives of main group elements.[8,11−16] These ligands have been used to stabilize cationic two-coordinate Ge(II) and Sn(II) species such as $\{[(i\text{-Pr})_2ATI]Ge\}^+$ and $\{[(i\text{-Pr})_2ATI]Sn\}^+$,[12,13]

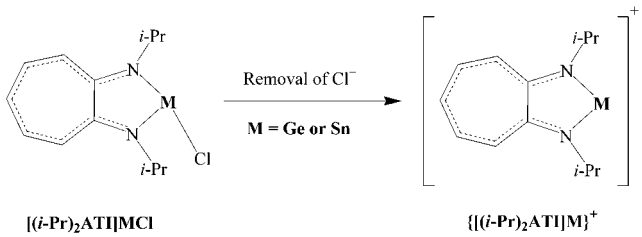

$[(i\text{-Pr})_2ATI]MCl$ $\{[(i\text{-Pr})_2ATI]M\}^+$

to our knowledge the first such compounds reported in the literature. The halide abstraction from the appropriate starting material is the most convenient approach to their synthesis. We have also investigated the utility of various counterions. Some weakly coordinating ions such as $[Cp(Cl)_2Zr(\mu\text{-}Cl)_3Zr(Cl)_2Cp]^-$ work well as counterions to cationic germanium species, while others like BPh_4^- react with the Ge^+ ion, resulting in various products, for example, $[(i\text{-Pr})_2ATI](Ph)Ge\rightarrow BPh_3$.[12]

In this paper, we report the results of our studies involving the use of silver derivatives of trifluoromethanesulfonate and highly fluorinated tris(pyrazoyl)borate $[HB(3,5\text{-}(CF_3)_2Pz)_3]^-$ (where $[HB(3,5\text{-}(CF_3)_2Pz)_3]^-$ = hydrotris(3,5-bis(trifluoromethyl)pyrazolyl)borate)[8,17−19] to abstract the chloride from $[(n\text{-Pr})_2ATI]GeCl$ and $[(n\text{-Pr})_2ATI]SnCl$ complexes. We show that the silver salt metathesis between CF_3SO_3Ag and $[(n\text{-Pr})_2ATI]GeCl$ or $[(n\text{-Pr})_2ATI]SnCl$ proceeds smoothly, while the halide abstraction does not occur when silver derivatives of $[HB(3,5\text{-}(CF_3)_2Pz)_3]^-$ are used. Instead, interesting adducts containing unsupported silver−germanium and silver−tin bonds have been isolated. Furthermore, the role of the halide has been investigated, as the synthesis of $[(n\text{-Pr})_2ATI]SnI$ and its reaction with $[HB(3,5\text{-}(CF_3)_2Pz)_3]Ag(\eta^2\text{-toluene})$ is reported. A brief account of our initial findings involving $[(Me)_2ATI]GeCl$ and silver salts of $[HB(3,5\text{-}(CF_3)_2Pz)_3]^-$ was reported.[8]

Experimental Section

General Procedures. All manipulations were carried out under an atmosphere of purified nitrogen either using standard Schlenk techniques or in a Vacuum Atmospheres single station drybox equipped with a −25 °C refrigerator. Solvents were purchased from commercial sources and distilled from conventional drying agents prior to use. Glassware was oven-dried at 150 °C overnight. The NMR spectra were recorded at room temperature on a JEOL Eclipse 500 (^1H, 500.16 MHz; ^{19}F, 470.62 MHz; ^{13}C, 125.78 MHz; ^{119}Sn, 186.5 MHz). Proton and carbon chemical shifts are reported in parts per million versus Me_4Si. ^{19}F and ^{119}Sn NMR chemical shifts were referenced to external $CFCl_3$ and Me_4Sn standards, respectively. Melting points were obtained on a Mel-Temp II apparatus. Elemental analyses were performed at the University of Texas at Arlington using a Perkin-Elmer Model 2400 CHN analyzer. Tropolone,[20] 2-(tosyloxy)tropone,[21] $GeCl_2\cdot$(1,4-dioxane),[22] and $[HB(3,5\text{-}(CF_3)_2Pz)_3]Ag(\eta^2\text{-toluene})$[19] were synthesized as reported previously. *n*-Propylamine, $Et_3O\cdot BF_4$, *n*-BuLi (1.6 M solution in hexane), $SnCl_2$, SnI_2, and $AgSO_3CF_3$ were obtained from commercial sources and used as received.

2-(*n*-Propylamino)tropone. Finely powdered 2-(tosyloxy)-tropone (5.00 g, 18 mmol; prepared from tropolone) was slowly added to *n*-propylamine (20 mL) at 0 °C. During the addition, the solution became dark red. After the addition, the solution was allowed to stir for 2 h at 0 °C. Then, the mixture was warmed to room temperature and stirred overnight. The excess *n*-propylamine was removed from the resulting yellow solution by distillation, and the resulting residue was dried under reduced pressure for 1 h. Extraction with diethyl ether, filtration through Celite, and removal of the diethyl ether under vacuum gave a brown liquid (2.90 g, 98%). ^1H NMR ($CDCl_3$): δ 1.02 (t, 3H, J = 7.5 Hz, $CH_3CH_2CH_2$), 1.74 (m, 2H, $CH_3CH_2CH_2$), 3.25 (m, 2H, $CH_3CH_2CH_2$), 6.51 (d, 1H, J = 10.5 Hz, H_7), 6.64 (t, 1H, J = 10.4 Hz, H_5), 7.13 (d, 1H, J = 11.5 Hz, H_3), 7.22 (m, 2H, $H_{4,6}$). $^{13}C\{^1H\}$ NMR ($CDCl_3$): δ 11.7 ($CH_3CH_2CH_2$), 21.7 ($CH_3CH_2CH_2$), 44.6 ($CH_3CH_2CH_2$), 108.6, 122.0, 128.2, 136.3, 137.2, 155.7, 176.5. IR (film, cm^{-1}): 3304 (N−H) (br,s), 3042 (w), 2963 (s), 2933 (w), 2875 (m), 1976 (w), 1654 (w), 1632 (w), 1602 (s), 1550 (w), 1511 (s), 1453 (s), 1406 (s), 1391 (m), 1259 (s), 1225 (m), 1213 (m), 1148 (m), 1084 (m), 1012 (m), 984 (w), 967 (w), 895 (w), 876 (s), 844 (w), 799 (w), 761 (m), 723 (s), 683 (w). Anal. Calcd for $C_{10}H_{13}N_2O$: C, 73.59; H, 8.03; N, 8.58. Found: C, 73.43; H, 7.76; N, 8.25.

***N*-(*n*-Propyl)-2-(*n*-propylamino)troponimine.** A methylene chloride solution of $Et_3O\cdot BF_4$ (1.34 g, 7.05 mmol) was slowly added to a methylene chloride solution of 2-(*n*-propylamino)tropone (1.15 g, 7.05 mmol) at room temperature. After stirring for 3 h, 20 mL of *n*-propylamine was added. The solution immediately turned yellow and got very warm. The reaction mixture was stirred for 2 more hours, and all volatiles were removed under vacuum. The residue was extracted into hexane and filtered through Celite. The removal of hexane under vacuum gave a yellow liquid. This liquid was then distilled under vacuum to obtain $[(n\text{-Pr})_2ATI]H$ as a yellow

(10) Liston, D. J.; Reed, C. A.; Eigenbrot, C. W.; Scheidt, W. R. *Inorg. Chem.* **1987**, *26*, 2739−40.
(11) Dias, H. V. R.; Wang, Z.; Jin, W. *Coord. Chem. Rev.* **1998**, *176*, 67−86.
(12) Dias, H. V. R.; Wang, Z. *J. Am. Chem. Soc.* **1997**, *119*, 4650−4655.
(13) Dias, H. V. R.; Jin, W. *J. Am. Chem. Soc.* **1996**, *118*, 9123−9126.
(14) Dias, H. V. R.; Jin, W.; Ratcliff, R. E. *Inorg. Chem.* **1995**, *34*, 6100−6105.
(15) Dias, H. V. R.; Jin, W. *Inorg. Chem.* **1996**, *35*, 6546−6551.
(16) Dias, H. V. R.; Jin, W.; Wang, Z. *Inorg. Chem.* **1996**, *35*, 6074−6079.
(17) Dias, H. V. R.; Jin, W.; Kim, H.-J.; Lu, H.-L. *Inorg. Chem.* **1996**, *35*, 2317−2328.
(18) Dias, H. V. R.; Lu, H.-L.; Ratcliff, R. E.; Bott, S. G. *Inorg. Chem.* **1995**, *34*, 1975−1976.
(19) Dias, H. V. R.; Jin, W.; Wang, Z. *Inorg. Chem.* **1997**, *36*, 6205−6215.
(20) Minns, R. A.; Elliott, A. J.; Sheppard, W. A. *Org. Synth.* **1977**, *57*, 117−121.
(21) Doering, W. v. E.; Hiskey, C. *J. Am. Chem. Soc.* **1952**, *74*, 5688−5693.
(22) Fjeldberg, T.; Haaland, A.; Schilling, B. E.; Lappert, M. F.; Thorne, A. J. *J. Chem. Soc., Dalton Trans.* **1986**, 1551−1556.

liquid (0.95 g, 66%) at 143−145 °C. ^{1}H NMR ($CDCl_3$): δ 1.00 (t, 6H, J = 7.5 Hz, $CH_3CH_2CH_2$), 1.73 (m, 4H, $CH_3CH_2CH_2$), 3.22 (t, 4H, J = 7.0 Hz, $CH_3CH_2CH_2$), 6.08 (t, 1H, J = 9.2 Hz, H_5), 6.23 (d, 2H, J = 11.0 Hz, $H_{3,7}$), 6.70 (m, 2H, $H_{4,6}$). $^{13}C\{^1H\}$ NMR ($CDCl_3$): δ 12.1 ($CH_3CH_2CH_2$), 23.3 ($CH_3CH_2CH_2$), 48.1 ($CH_3CH_2CH_2$), 110.0 (C_5), 117.4 ($C_{3,7}$), 132.8 ($C_{4,6}$), 152.9 ($C_{2,8}$). IR (film, cm^{-1}): 3218 (N−H) (br,m), 2960 (s), 2929 (w), 2871 (m), 1931 (w), 1634 (w), 1590 (s), 1510 (s), 1465 (s), 1428 (w), 1415 (w), 1386 (s), 1270 (s), 1205 (m), 1147 (m), 1100 (w), 966 (s), 901 (w), 881 (s), 859 (w), 815 (w), 744 (m), 702 (s), 625 (w). Anal. Calcd for $C_{13}H_{20}N_2$: C, 76.42; H, 9.87; N, 13.71. Found: C, 76.26; H, 9.53; N, 13.23.

[(*n*-Pr)$_2$ATI]GeCl. A diethyl ether solution (20 mL) of [(*n*-Pr)$_2$ATI]H (500 mg, 2.45 mmol) was treated with *n*-BuLi (1.53 mL, 1.6 M hexane solution) at −78 °C. The solution became cloudy orange. It was stirred for 0.5 h, warmed to room temperature, and stirred for an additional 0.5 h. This solution was then slowly added to a suspension of $GeCl_2$·(1,4-dioxane) (570 mg, 2.45 mmol) in diethyl ether (15 mL) at −78 °C. The mixture immediately turned red. The low temperature was maintained for one further hour, and then the mixture was allowed to warm to room temperature and stirred overnight. After overnight stirring, all volatiles were removed under vacuum. The remaining solid was extracted into toluene and filtered through Celite. The toluene was removed under vacuum to yield a yellow-orange solid (730 mg, 96%). Recrystallization from toluene at room temperature gave X-ray quality crystals. Mp: 93−95 °C. ^{1}H NMR ($CDCl_3$): δ 1.05 (t, 6H, J = 7.3 Hz, $CH_3CH_2CH_2$), 1.95 (m, 4H, $CH_3CH_2CH_2$), 3.64 (m, 4H, $CH_3CH_2CH_2$), 6.75 (t, 1H, J = 9.4 Hz, H_5), 6.84 (d, 2H, J = 11.2 Hz, $H_{3,7}$), 7.32 (m, 2H, $H_{4,6}$). $^{13}C\{^1H\}$ NMR ($CDCl_3$): δ 12.0 ($CH_3CH_2CH_2$), 22.3 ($CH_3CH_2CH_2$), 48.2 ($CH_3CH_2CH_2$), 115.6 (C_5), 123.3 ($C_{3,7}$), 136.8 ($C_{4,6}$), 160.3 ($C_{2,8}$). Anal. Calcd for $C_{13}H_{19}N_2GeCl$: C, 50.15; H, 6.15; N, 9.00. Found: C, 49.76; H, 5.86; N, 8.44.

[(*n*-Pr)$_2$ATI]SnCl. A diethyl ether solution (30 mL) of [(*n*-Pr)$_2$ATI]H (1.00 g, 4.89 mmol) was treated with *n*-BuLi (3.06 mL, 1.6 M hexane solution) at −78 °C. The solution became cloudy orange. It was stirred for 0.5 h, warmed to room temperature, and stirred for an additional 0.5 h. This solution was then slowly added to a suspension of $SnCl_2$ (930 mg, 4.89 mmol) in diethyl ether (20 mL) at −78 °C. The mixture immediately turned orange. The low temperature was maintained for one further hour, and then the mixture was allowed to warm to room temperature and stirred overnight. After overnight stirring, all volatiles were removed under vacuum. The remaining solid was extracted into toluene and filtered through Celite. The toluene was removed under vacuum to yield a red-orange solid (1.09 g, 62%). Recrystallization from toluene at room temperature gave X-ray quality crystals. Mp: 104−105 °C. ^{1}H NMR ($CDCl_3$): δ 1.08 (t, 6H, J = 7.2 Hz, $CH_3CH_2CH_2$), 2.03 (m, 4H, $CH_3CH_2CH_2$), 3.60 (m, 4H, $CH_3CH_2CH_2$), 6.63 (t, 1H, J = 9.3 Hz, H_5), 6.74 (d, 2H, J = 11.3 Hz, $H_{3,7}$), 7.25 (m, 2H, $H_{4,6}$). $^{13}C\{^1H\}$ NMR ($CDCl_3$): δ 12.3 ($CH_3CH_2CH_2$), 24.1 ($CH_3CH_2CH_2$), 50.6 ($CH_3CH_2CH_2$), 115.5 (C_5), 121.7 ($C_{3,7}$), 135.9 ($C_{4,6}$), 163.0 ($C_{2,8}$). $^{119}Sn\{^1H\}$ NMR ($CDCl_3$): δ −84. Anal. Calcd for $C_{13}H_{19}N_2SnCl$: C, 43.68; H, 5.36; N, 7.84. Found: C, 43.74; H, 4.97; N, 7.15.

{[(*n*-Pr)$_2$ATI]Ge}[SO$_3$CF$_3$]. [(*n*-Pr)$_2$ATI]GeCl (110 mg, 0.35 mmol) and $AgSO_3CF_3$ (90 mg, 0.35 mmol) were mixed in dichloromethane (10 mL) at room temperature. The mixture immediately became cloudy yellow. It was stirred for 30 min and filtered through Celite. Removal of the dichloromethane under vacuum and recrystallization of the resulting solid from toluene at −25 °C gave crystals of the yellow product (130 mg, 87%). X-ray quality crystals were grown from toluene at room temperature. Mp: 138−140 °C. ^{1}H NMR ($CDCl_3$): δ 1.04 (t, 6H, J = 7.3 Hz, $CH_3CH_2CH_2$), 1.97 (m, 4H, $CH_3CH_2CH_2$), 3.87 (m, 4H, $CH_3CH_2CH_2$), 7.19 (t, 1H, J = 9.5 Hz, H_5), 7.26 (d, 2H, J = 11.0 Hz, $H_{3,7}$), 7.66 (m, 2H, $H_{4,6}$). ^{19}F NMR ($CDCl_3$): δ −77.84 (s, CF_3). $^{13}C\{^1H\}$ NMR ($CDCl_3$): δ 11.6 ($CH_3CH_2CH_2$), 22.5 ($CH_3CH_2CH_2$), 48.5 ($CH_3CH_2CH_2$), 118.3 (C_5), 119.4 (q, CF_3, J(C,F) = 319 Hz), 128.0 ($C_{3,7}$), 138.3 ($C_{4,6}$), 159.4 ($C_{2,8}$). Anal. Calcd for $C_{14}H_{19}F_3N_2O_3SGe$: C, 39.57; H, 4.51; N, 6.59. Found: C, 39.11; H, 4.53; N, 6.22.

{[(*n*-Pr)$_2$ATI]Sn}[SO$_3$CF$_3$]. [(*n*-Pr)$_2$ATI]SnCl (200 mg, 0.56 mmol) and $AgSO_3CF_3$ (145 mg, 0.56 mmol) were mixed in dichloromethane (10 mL) at room temperature. The mixture immediately became cloudy yellow. It was stirred for 30 min and filtered through Celite. The filtrate was concentrated and cooled to −25 °C to obtain yellow crystals (185 mg, 71%). X-ray quality crystals were grown from dichloromethane at room temperature. Mp: 171−173 °C. ^{1}H NMR ($CDCl_3$): δ 1.12 (t, 6H, J = 7.3 Hz, $CH_3CH_2CH_2$), 2.06 (m, 4H, $CH_3CH_2CH_2$), 3.73 (m, 4H, $CH_3CH_2CH_2$), 6.91 (t, 1H, J = 9.3 Hz, H_5), 6.99 (d, 2H, J = 11.3 Hz, $H_{3,7}$), 7.47 (m, 2H, $H_{4,6}$). ^{19}F NMR ($CDCl_3$): δ −78.01 (s, CF_3). $^{13}C\{^1H\}$ NMR ($CDCl_3$): δ 12.3 ($CH_3CH_2CH_2$), 24.7 ($CH_3CH_2CH_2$), 50.9 ($CH_3CH_2CH_2$), 116.6 (C_5), 119.6 (q, CF_3, J(C,F) = 319 Hz), 124.6 ($C_{3,7}$), 136.4 ($C_{4,6}$), 163.3 ($C_{2,8}$). Anal. Calcd for $C_{14}H_{19}F_3N_2O_3SSn$: C, 35.69; H, 4.07; N, 5.95. Found: C, 35.54; H, 4.11; N, 5.87.

[HB(3,5-(CF$_3$)$_2$Pz)$_3$]Ag←Ge(Cl)[(*n*-Pr)$_2$ATI]. [(*n*-Pr)$_2$ATI]GeCl (57 mg, 0.18 mmol) and [HB(3,5-(CF$_3$)$_2$Pz)$_3$]Ag(η^2-toluene) (150 mg, 0.18 mmol) were mixed in dichloromethane (10 mL) at room temperature. After the solution was stirred for 2 h, the solvent was removed under vacuum and the resulting solid was dissolved in toluene. Filtration through Celite and removal of the toluene under vacuum gave the yellow product (180 mg, 95%). X-ray quality crystals were grown from hexane at room temperature. Mp: decomposed around 160 °C. ^{1}H NMR ($CDCl_3$): δ 1.02 (t, 6H, J = 7.5 Hz, $CH_3CH_2CH_2$), 1.82 (m, 2H, $CH_3CH_2CH_2$), 1.90 (m, 2H, $CH_3CH_2CH_2$), 3.73 (m, 4H, $CH_3CH_2CH_2$), 6.89 (s, 3H, Pz-CH), 6.98 (t, 1H, J = 9.5 Hz, H_5), 7.03 (d, 2H, J = 11.3 Hz, $H_{3,7}$), 7.50 (m, 2H, $H_{4,6}$). ^{19}F NMR ($CDCl_3$): δ −58.65 (d, ^5J(F,H) = 2.2 Hz), −60.84 (d, ^4J(F,Ag) = 2.2 Hz). $^{13}C\{^1H\}$ NMR ($CDCl_3$): δ 11.3 ($CH_3CH_2CH_2$), 21.7 ($CH_3CH_2CH_2$), 47.2 ($CH_3CH_2CH_2$), 106.3 (CH), 116.9 (C_5), 119.3 (q, ^1J(C,F) = 270.6 Hz, CF_3), 120.4 (q, ^1J(C,F) = 269.8 Hz, CF_3), 125.5 ($C_{3,7}$), 138.3 ($C_{4,6}$), 140.1 (q, ^2J(C,F) = 40.1 Hz, CCF_3), 143.6 (q, ^2J(C,F) = 38.1 Hz, CCF_3), 158.9 ($C_{2,8}$). Anal. Calcd for $C_{28}H_{23}F_{18}N_8BAgGeCl$: C, 32.33; H, 2.23; N, 10.77. Found: C, 31.96; H, 2.20; N, 10.39.

[HB(3,5-(CF$_3$)$_2$Pz)$_3$]Ag←Sn(Cl)[(*n*-Pr)$_2$ATI]. [(*n*-Pr)$_2$ATI]SnCl (60 mg, 0.17 mmol) and [HB(3,5-(CF$_3$)$_2$Pz)$_3$]Ag(η^2-toluene) (140 mg, 0.17 mmol) were mixed in dichloromethane (10 mL) at room temperature. After the solution was stirred for 2 h, the solvent was removed under vacuum and the resulting solid was dissolved in toluene. Filtration through Celite and removal of the toluene under vacuum gave the yellow product (170 mg, 94%). X-ray quality crystals were grown from hexane at room temperature. Mp: decomposed around 150 °C. ^{1}H NMR ($CDCl_3$): δ 1.06 (t, 6H, J = 7.3 Hz, $CH_3CH_2CH_2$), 1.98 (m, 4H, $CH_3CH_2CH_2$), 3.69 (m, 4H, $CH_3CH_2CH_2$), 6.88 (t, 1H, J = 9.5 Hz, H_5), 6.92 (s, 3H, Pz-CH), 6.99 (d, 2H, J = 11.5 Hz, $H_{3,7}$), 7.44 (m, 2H, $H_{4,6}$). ^{19}F NMR ($CDCl_3$): δ −58.68 (d, ^5J(F,H) = 3.2 Hz), −60.72 (s). $^{13}C\{^1H\}$ NMR ($CDCl_3$): δ 11.6 ($CH_3CH_2CH_2$), 23.5 ($CH_3CH_2CH_2$), 50.1 ($CH_3CH_2CH_2$), 106.4 (CH), 116.9 (C_5), 119.2 (q, ^1J(C,F) = 270.6 Hz, CF_3), 120.4 (q, ^1J(C,F) = 269.8 Hz, CF_3), 124.3 ($C_{3,7}$), 137.2 ($C_{4,6}$), 140.3 (q, ^2J(C,F) = 40.1 Hz, CCF_3), 143.6 (q, ^2J(C,F) = 38.4 Hz, CCF_3), 161.4 ($C_{2,8}$). $^{119}Sn\{^1H\}$ NMR ($CDCl_3$): δ 117 (d,

^1J(Sn,Ag) = 5234 Hz). Anal. Calcd for $C_{28}H_{23}F_{18}N_8BAgSnCl$: C, 30.96; H, 2.13; N, 10.31. Found: C, 30.85; H, 2.08; N, 9.87.

[(*n*-Pr)$_2$ATI]SnI. A diethyl ether solution (30 mL) of [(*n*-Pr)$_2$ATI]H (250 mg, 1.22 mmol) was treated with *n*-BuLi (0.76 mL, 1.6 M hexane solution) at −78 °C. The solution became cloudy orange. It was stirred for 0.5 h, warmed to room temperature, and stirred for an additional 0.5 h. This solution was then slowly added to a suspension of SnI_2 (456 mg, 1.22 mmol) in diethyl ether (20 mL) at −78 °C. The mixture immediately turned bright orange. The low temperature was maintained for one further hour, and then the mixture was allowed to warm to room temperature and stirred overnight. After overnight stirring, all volatiles were removed under vacuum. The remaining solid was extracted into warm toluene−dichloromethane (1:1) and filtered through Celite. All volatiles were removed under vacuum to yield a red solid (410 mg, 75%). Recrystallization from toluene−dicloromethane (1:1) at room temperature gave X-ray quality crystals. Mp: 156−160 °C. ^{1}H NMR ($CDCl_3$): δ 1.08 (t, 6H, J = 7.3 Hz, $CH_3CH_2CH_2$), 2.05 (m, 4H, $CH_3CH_2CH_2$), 3.57 (m, 4H, $CH_3CH_2CH_2$), 6.67 (t, 1H, J = 9.3 Hz, H_5), 6.76 (d, 2H, J = 11.3 Hz, $H_{3,7}$), 7.26 (m, 2H, $H_{4,6}$). ^{13}C{^{1}H} NMR ($CDCl_3$): δ 12.2 ($CH_3CH_2CH_2$), 23.5 ($CH_3CH_2CH_2$), 50.8 ($CH_3CH_2CH_2$), 116.4 (C_5), 122.2 ($C_{3,7}$), 136.0 ($C_{4,6}$), 163.2 ($C_{2,8}$). ^{119}Sn{^{1}H} NMR ($CDCl_3$): δ 19. Anal. Calcd for $C_{13}H_{19}N_2SnI$: C, 34.78; H, 4.27; N, 6.24. Found: C, 34.52; H, 4.28; N, 6.07.

[HB(3,5-(CF$_3$)$_2$Pz)$_3$]Ag−Sn(I)[(*n*-Pr)$_2$ATI]. [(*n*-Pr)$_2$ATI]SnI (80 mg, 0.18 mmol) and [HB(3,5-(CF$_3$)$_2$Pz)$_3$]Ag(η^2-toluene) (150 mg, 0.18 mmol) were mixed in dichloromethane (10 mL) at room temperature. After the solution was stirred for 2 h, the solvent was removed under vacuum and the resulting solid was dissolved in hexane. Filtration through Celite and removal of the hexane under vacuum gave the yellow product (190 mg, 91%). X-ray quality crystals were grown from hexane at −25 °C. Mp: 122−124 °C. ^{1}H NMR ($CDCl_3$): δ 1.05 (t, 6H, J = 7.2 Hz, $CH_3CH_2CH_2$), 1.99 (m, 4H, $CH_3CH_2CH_2$), 3.66 (m, 4H, $CH_3CH_2CH_2$), 6.86 (t, 1H, J = 9.2 Hz, H_5), 6.91 (s, 3H, Pz-CH), 6.94 (d, 2H, J = 11.5 Hz, $H_{3,7}$), 7.41 (m, 2H, $H_{4,6}$). ^{19}F NMR ($CDCl_3$): δ −58.68 (d, ^5J(F,H) = 2.2 Hz), −60.84 (s). ^{13}C{^{1}H} NMR ($CDCl_3$): δ 11.7 ($CH_3CH_2CH_2$), 23.1 ($CH_3CH_2CH_2$), 50.3 ($CH_3CH_2CH_2$), 106.4 (CH), 117.5 (C_5), 119.3 (q, ^1J(C,F) = 270.8 Hz, CF_3), 120.4 (q, ^1J(C,F) = 270.0 Hz, CF_3), 124.3 ($C_{3,7}$), 137.1 ($C_{4,6}$), 140.3 (q, ^2J(C,F) = 40.0 Hz, CCF_3), 143.6 (q, ^2J(C,F) = 38.2 Hz, CCF_3), 161.6 ($C_{2,8}$). ^{119}Sn-{^{1}H} NMR ($CDCl_3$): δ 111 (d, ^1J(Sn,Ag) = 4359 Hz). Anal. Calcd for $C_{28}H_{23}F_{18}N_8BAgSnI$: C, 28.55; H, 1.97; N, 9.51. Found: C, 28.64; H, 1.93; N, 9.38.

X-ray Structure Determination. A suitable crystal covered with a layer of hydrocarbon oil was selected and attached to a glass fiber and immediately placed in the low-temperature nitrogen stream.[23] Data collections were carried out at low temperature on a Siemens P4 diffractometer equipped with a LT-2A device for low-temperature work and graphite monochromated Mo Kα radiation (λ = 0.710 73 Å). Three standard reflections were measured at intervals of every 97 data points to check for crystal deterioration and/or misalignment. No significant deterioration in intensity was observed. Data were corrected for Lorentz, polarization, and absorption (using ψ scans) effects. Structures were solved by direct methods, followed by successive cycles of full-matrix least-squares refinement on F^2 and difference Fourier analysis. Software programs and the sources of scattering factors are contained in the Bruker SHELXTL 5.1 software package provided by the Bruker Analytical X-ray Instruments, Inc.[24] Cell dimensions and structure refinement data for all the germanium and tin complexes are listed in Table 1. Selected bond lengths and angles are given in the figure captions.

Scheme 1. Synthesis of aminotroponiminatogermanium(II) and tin(II) chloro derivatives.

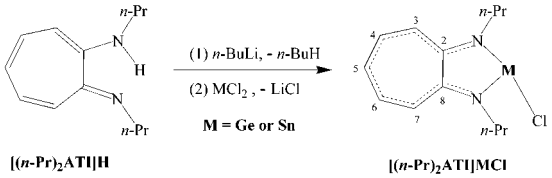

Results and Discussion

The *N*-(*n*-propyl)-2-(*n*-propylamino)troponimine, [(*n*-Pr)$_2$-ATI]H,[25] was synthesized by a two-step procedure similar to the procedures for [(*i*-Pr)$_2$ATI]H[14] and [(Me)$_2$ATI]H[15] and isolated in about 66% overall yield. The first step involves the direct nucleophilic displacement of the tosyl group on the 2-(tosyloxy)tropone using excess *n*-propylamine. The *N*-(*n*-propylamino)tropone was isolated in quantitative yield. The second step involves the ethylation of *N*-(*n*-propyl)-aminotropone with $Et_3O{\cdot}BF_4$ followed by treatment with excess *n*-propylamine to obtain analytically pure [(*n*-Pr)$_2$-ATI]H as a bright yellow solid. The ^{1}H NMR spectrum shows three well-defined sets of multiplets in the aromatic region, which can be assigned to H(5), H(3,7), and H(4,6), indicating the presence of a C_2 symmetric species in solution (see Scheme 1 for numbering method). The ^{13}C NMR spectrum shows only four signals corresponding to the ring carbons C(2,8), C(4,6), C(3,7), and C(5). The carbons attached to the amine and imine groups (that is, C(2,8)) appear as a single peak at 152.9 ppm in the ^{13}C NMR spectrum. These data suggest [(*n*-Pr)$_2$ATI]H to be in a rapid tautomeric equilibrium in solution. The N−H absorption of [(*n*-Pr)$_2$ATI]H appears in the IR spectrum at 3218 cm^{-1}. These NMR chemical shift values and IR data agree well with those for [(*i*-Pr)$_2$ATI]H and [(Me)$_2$ATI]H.[14,15]

Synthesis of [(*n*-Pr)$_2$ATI]GeCl or [(*n*-Pr)$_2$ATI]SnCl was achieved by the treatment of $GeCl_2{\cdot}$(1,4-dioxane) or $SnCl_2$ with [(*n*-Pr)$_2$ATI]Li in a 1:1 molar ratio in Et_2O. They were isolated as orange solids in good yields and characterized by ^{1}H and ^{13}C NMR spectroscopy and by X-ray diffraction. ^{1}H and ^{13}C NMR data indicate a C_2 symmetric solution structure for the [(*n*-Pr)$_2$ATI]$^-$ moiety of the two chloro adducts [(*n*-Pr)$_2$ATI]GeCl and [(*n*-Pr)$_2$ATI]SnCl. For example, the ^{1}H NMR spectrum of [(*n*-Pr)$_2$ATI]GeCl taken in $CDCl_3$ shows three well-separated multiplets which correspond to H(5), H(3,7), and H(4,6) of the seven-membered ring. The ^{13}C NMR spectrum displays four resonances for the ring carbons. Compared to the case of the free ligand [(*n*-Pr)$_2$ATI]H, the ^{1}H NMR signals due to the ring protons of [(*n*-Pr)$_2$ATI]GeCl and [(*n*-Pr)$_2$ATI]SnCl show a significant downfield shift. This may be a result of the increased conjugation of π-electrons in the newly formed metallacycles.

(23) Hope, H. In *Experimental Organometallic Chemistry;* Wayda, A. L., Darensbourg, M. Y., Eds.; ACS Symposium Series, No. 357; American Chemical Society: Washington, DC, 1987; p 257.

(24) *SHELXTL*, version 5.1; Bruker Analytical X-ray Systems, Inc.: Madison, WI, 1997.

(25) Mimata, Y.; Saisho, T.; Hamada, M.; Imafuku, K. *J. Chem. Res., Synop.* **1995**, 156.

Table 1. Crystal Data and Summary of Data Collection and Refinement for Compounds [(*n*-Pr)$_2$ATI]GeCl, [(*n*-Pr)$_2$ATI]SnCl, {[(*n*-Pr)$_2$ATI]Ge}[SO$_3$CF$_3$], {[(*n*-Pr)$_2$ATI]Sn}[SO$_3$CF$_3$], [HB(3,5-(CF$_3$)$_2$Pz)$_3$]Ag←Ge(Cl)[(*n*-Pr)$_2$ATI], [HB(3,5-(CF$_3$)$_2$Pz)$_3$]Ag←Sn(Cl)[(*n*-Pr)$_2$ATI], [HB(3,5-(CF$_3$)$_2$Pz)$_3$]Ag←Sn(I)[(*n*-Pr)$_2$ATI]

	[(*n*-Pr)$_2$ATI]GeCl	[(*n*-Pr)$_2$ATI]SnCl	{[(*n*-Pr)$_2$ATI]Ge}-[SO$_3$CF$_3$]	{[(*n*-Pr)$_2$ATI]Sn}-[SO$_3$CF$_3$]	[HB(3,5-(CF$_3$)$_2$Pz)$_3$]Ag←Ge(Cl)[(*n*-Pr)$_2$ATI]	[HB(3,5-(CF$_3$)$_2$Pz)$_3$]Ag←Sn(Cl)[(*n*-Pr)$_2$ATI]	[(*n*-Pr)$_2$ATI]SnI	[HB(3,5-(CF$_3$)$_2$Pz)$_3$]Ag←Sn(I)[(*n*-Pr)$_2$ATI]
formula	$C_{13}H_{19}ClGeN_2$	$C_{13}H_{19}ClN_2Sn$	$C_{14}H_{19}F_3GeN_2O_3S$	$C_{14}H_{19}F_3N_2O_3SSn$	$C_{28}H_{23}AgBClF_{18}GeN_8$	$C_{28}H_{23}AgBClF_{18}N_8Sn$	$C_{13}H_{19}IN_2Sn$	$C_{34}H_{37}AgBF_{18}IN_8Sn$
fw	311.34	357.44	424.96	471.06	1040.26	1086.36	448.89	1263.99
space group	$P\bar{1}$	$P\bar{1}$	$P2_1/m$	$P2_1/m$	$P2_1/c$	$P\bar{1}$	$P\bar{1}$	$P2_1/c$
T, K	198(2)	198(2)	213(2)	208(2)	213(2)	213(2)	213(2)	208(2)
λ, Å	0.710 73	0.710 73	0.710 73	0.710 73	0.710 73	0.710 73	0.710 73	0.71073
a, Å	7.6768(14)	8.4329(8)	10.558(3)	10.5691(15)	13.0623(19)	9.7302(15)	8.5771(7)	22.835(6)
b, Å	9.7088(10)	9.7698(11)	7.3127(5)	7.3568(17)	17.0073(18)	12.0720(12)	9.9182(9)	11.5989(15)
c, Å	10.9671(18)	18.6523(15)	11.3595(13)	11.5109(7)	17.095(2)	16.9259(11)	18.8976(13)	17.228(3)
α, deg	115.823(12)	80.867(7)	90	90	90	88.117(6)	80.296(6)	90
β, deg	96.971(15)	78.742(8)	90.348(19)	90.513(11)	90.652(14)	86.438(9)	80.879(8)	91.082(15)
γ, deg	103.919(13)	72.340(10)	90	90	90	78.428(9)	73.331(11)	90
V, Å^3	689.84(18)	1428.0(2)	877.0(3)	895.0(3)	3797.6(9)	1943.6(4)	1507.6(2)	4562.3(16)
Z	2	4	2	2	4	2	4	4
ρ(calc), g/cm^3	1.499	1.663	1.609	1.748	1.819	1.856	1.978	1.840
μ, mm^{-1}	2.394	1.958	1.910	1.588	1.500	1.335	3.725	1.763
R1, wR2 [$I > 2\sigma(I)$]^a	0.0215, 0.0557	0.0239, 0.0628	0.0342, 0.0872	0.0321, 0.0806	0.0326, 0.0797	0.0390, 0.0904	0.0303, 0.0760	0.0464, 0.1063
R1, wR2 (all data)^a	0.0219, 0.0560	0.0269, 0.0644	0.0403, 0.0915	0.0355, 0.0825	0.0379, 0.0826	0.0452, 0.0950	0.0344, 0.0783	0.0748, 0.1200

^{a} R1 = $\sum||F_o| - |F_c||/\sum|F_o|$ and wR2 = $[\sum[w(F_o^2 - F_c^2)^2]/\sum[w(F_o^2)^2]]^{1/2}$.

Figure 1. Representation of the X-ray crystal structure of [(*n*-Pr)$_2$ATI]-GeCl (hydrogen atoms not shown). Selected bond lengths (Å) and angles (deg) are as follows: Ge−N(1), 1.924(2); Ge−N(9), 1.949(2); Ge−Cl, 2.3776(8); N(1)−C(2), 1.345(3); N(1)−C(10), 1.468(3); N(9)−C(8), 1.334(3); N(9)−C(13), 1.472(3); N(1)−Ge−N(9), 80.24(8); N(1)−Ge−Cl, 96.85(6); N(9)−Ge−Cl, 96.14(6); C(2)−N(1)−C(10), 122.2(2); C(2)−N(1)−Ge, 117.88(16); C(10)−N(1)−Ge, 119.88(16); C(8)−N(9)−C(13), 120.3(2); C(8)−N(9)−Ge, 116.94(16); C(13)−N(9)−Ge, 122.72(16).

The C(2,8) resonances show the most notable change in the ^{13}C spectra. The signals due to C(2,8) of [(*n*-Pr)$_2$ATI]GeCl and [(*n*-Pr)$_2$ATI]SnCl appear at about 7 and 10 ppm downfield from that of the free ligand [(*n*-Pr)$_2$ATI]H (δ 152.9).

The ^{119}Sn NMR spectrum of [(*n*-Pr)$_2$ATI]SnCl shows a signal at δ −84. This resonance appears at the region expected for three-coordinate tin atoms, for example, [(*i*-Pr)$_2$ATI]SnCl, δ −68;[13] [(Mes)$_2$DAP]SnCl (where [(Mes)$_2$-DAP] = 2,4-dimethyl-*N*,*N*′-bis(2,4,6-trimethylphenyl)-1,5-diazapentadienyl),[26] δ −236; [(Dipp)$_2$DAP]SnCl (where [(Dipp)$_2$DAP] = 2,4-dimethyl-*N*,*N*′-bis(2,6-diisopropylphenyl)-1,5-diazapentadienyl),[27] δ −224; and [H$_2$B(Pz)$_2$]-SnCl, δ −307.[28] Two-coordinate tin(II) adducts show ^{119}Sn signals at significantly higher chemical shift values (e.g., {[(*i*-Pr)$_2$ATI]Sn}$^+$,[13] δ 734; [(Me$_3$Si)$_2$N]$_2$Sn, δ 776)[29] whereas four-coordinate chloro tin(II) complexes show ^{119}Sn signals at relatively upfield regions (e.g., [HB(Pz)$_3$]SnCl, δ −569; [HB(3,5-Me$_2$Pz)$_3$]SnCl, δ −567).[28]

The X-ray crystal structure of [(*n*-Pr)$_2$ATI]GeCl is shown in Figure 1. The germanium center adopts a pyramidal geometry which is fairly common in Ge(II) chemistry. The sum of the bond angles at the germanium atom is 273°. The heterobicyclic C$_7$N$_2$Ge ring system is planar (mean deviation from the plane = 0.02 Å) and shows C_2 symmetry consistent with the NMR data. There are no significant intermolecular Ge···Ge or Ge···Cl contacts between neighboring [(*n*-Pr)$_2$ATI]GeCl molecules. The X-ray crystal structure of [(*n*-Pr)$_2$ATI]SnCl is depicted in Figure 2. The asymmetric unit contains two chemically similar but crystallographically different molecules. The tin center adopts a pyramidal

(26) Ayers, A. E.; Klapotke, T. M.; Dias, H. V. R. *Inorg. Chem.* **2001**, *40*, 1000−1005.
(27) Ding, Y.; Roesky, H. W.; Noltemeyer, M.; Schmidt, H.-G.; Power, P. P. *Organometallics* **2001**, *20*, 1190−1194.
(28) Reger, D. L.; Knox, S. J.; Huff, M. F.; Rheingold, A. L.; Haggerty, B. S. *Inorg. Chem.* **1991**, *30*, 1754−1759.
(29) Wrackmeyer, B.; Horchler, K.; Zhou, H. *Spectrochim. Acta* **1990**, *46A*, 809−816.

Table 2. Selected Bond Distances (Å) and Angles (deg) (X = Halide Ion or O; C_{ring} Refers to Values Related to the ATI Ring)[a]

	[(Me)$_2$ATI]-GeCl	[(*n*-Pr)$_2$ATI]-GeCl	[(*i*-Pr)$_2$ATI]-GeCl	{[(*n*-Pr)$_2$ATI]Ge}-[CF_3SO_3]	{[(*i*-Pr)$_2$ATI]Ge}-[CF_3SO_3]	{[(*i*-Pr)$_2$ATI]Ge}$^+$	[(Mes)$_2$DAP]-GeCl	[(Dipp)$_2$DAP]-GeCl
Ge−X	2.377(1)	2.3776(8)	2.368(2)	2.483	2.255(2)		2.328(1)	2.295(12)
Ge−N	1.937(3)	1.936(2)	1.956(4)	1.924(5)	1.913(2)	1.909(5)	1.969(2)	1.990(2)
N−C_{ring}	1.342(4)	1.340(3)	1.341(6)	1.354(7)	1.353(3)	1.347(8)		
N−Ge−N	80.1(1)	80.24(8)	80.3(2)	81.4(2)	81.79(8)	81.7(2)	90.44(9)	90.89(10)
ref	12	this work	12	this work	12	12	26	27

	[(Me)$_2$ATI]-SnCl	[(*n*-Pr)$_2$ATI]-SnCl	[(*i*-Pr)$_2$ATI]-SnCl	[(*n*-Pr)$_2$ATI]-SnI	{[(*n*-Pr)$_2$ATI]Sn}-[CF_3SO_3]	{[(*i*-Pr)$_2$ATI]Sn}$^+$	[(Mes)$_2$DAP]-SnCl	[(Dipp)$_2$DAP]-SnCl
Sn−X	2.514(1)	2.504(1)	2.542(2)	2.9073(7)	2.513(4)		2.468(1)	2.473(9)
Sn−N	2.140(3)	2.154(3)	2.164(5)	2.149(5)	2.128(5)	2.147(3)	2.162(3)	2.183(2)
N−C_{ring}	1.342(4)	1.336(5)	1.332(7)	1.326(7)	1.341(8)	1.338(5)		
N−Sn−N	73.7(1)	73.9(1)	73.9(2)	74.2(1)	75.0(2)	74.5(1)	87.38(17)	85.21(8)
ref	unpublished work	this work	13	this work	this work	13	26	27

[a] Average values are given for parameters involving more than one value.

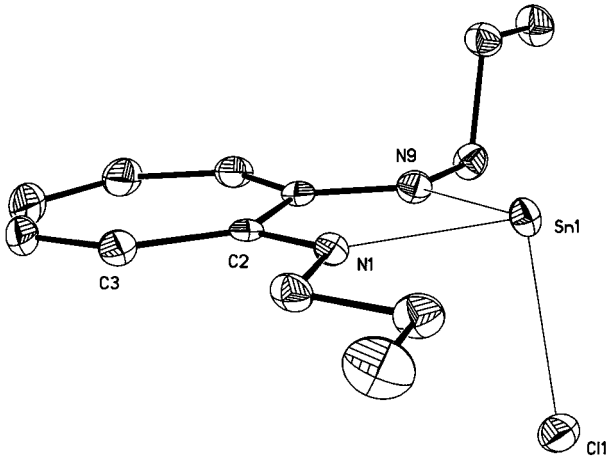

Figure 2. Representation of the X-ray crystal structure of [(*n*-Pr)$_2$ATI]-SnCl (hydrogen atoms and the second molecule in the asymmetric unit not shown). Selected bond lengths (Å) and angles (deg) are as follows. *Molecule 1*: Sn(1)−N(9), 2.146(3); Sn(1)−N(1), 2.157(3); Sn(1)−Cl(1), 2.4907(11); N(1)−C(2), 1.339(5); N(1)−C(10), 1.462(5); N(9)−C(8), 1.334(5); N(9)−C(13), 1.465(4); N(9)−Sn(1)−N(1), 74.10(11); N(9)−Sn(1)−Cl(1), 92.53(9); N(1)−Sn(1)−Cl(1), 94.59(8); C(2)−N(1)−C(10), 120.6(3); C(2)−N(1)−Sn(1), 118.1(2); C(10)−N(1)−Sn(1), 121.4(2); C(8)−N(9)−C(13), 122.4(3); C(8)−N(9)−Sn(1), 118.6(2); C(13)−N(9)−Sn(1), 119.0(2). *Molecule 2*: Sn(2)−N(16), 2.154(3); Sn(2)−N(24), 2.158(3); Sn(2)−Cl(2), 2.5176(13); N(16)−C(17), 1.335(5); N(16)−C(25), 1.477(4); N(24)−C(23), 1.337(5); N(24)−C(28), 1.479(5); N(16)−Sn(2)−N(24), 73.74(10); N(16)−Sn(2)−Cl(2), 91.77(9); N(24)−Sn(2)−Cl(2), 93.62(8); C(17)−N(16)−C(25), 120.1(3); C(17)−N(16)−Sn(2), 118.6(2); C(25)−N(16)−Sn(2), 121.3(2); C(23)−N(24)−C(28), 120.3(3); C(23)−N(24)−Sn(2), 118.4(2); C(28)−N(24)−Sn(2), 121.3(2).

geometry. Heterobicyclic C_7N_2Sn skeletons are planar (mean deviation from the plane = 0.01 and 0.03 Å for the two molecules in the asymmetric unit). The X-ray structure of the *N*-isopropyl isomer [(*i*-Pr)$_2$ATI]SnCl has been reported. However, in contrast to [(*i*-Pr)$_2$ATI]SnCl,[13] [(*n*-Pr)$_2$ATI]SnCl does not show intermolecular Sn···Cl contacts. The closest intermolecular Sn···Cl and Sn···Sn separations of [(*n*-Pr)$_2$ATI]SnCl are 4.31 and 3.54 Å, respectively.

Some key structural parameters of aminotroponiminato germanium and tin adducts are listed in Table 2. Overall, despite the size difference in the *N*-alkyl group, for a given M (where M = Ge or Sn), M−X and M−N bond distances and N−M−N angles are similar between the [(Me)$_2$ATI]-MCl, [(*n*-Pr)$_2$ATI]MCl, and [(*i*-Pr)$_2$ATI]MCl systems (where M = Ge or Sn).[12,13] Compared to the germanium derivatives,

Scheme 2. Silver salt metathesis using CF_3SO_3Ag.

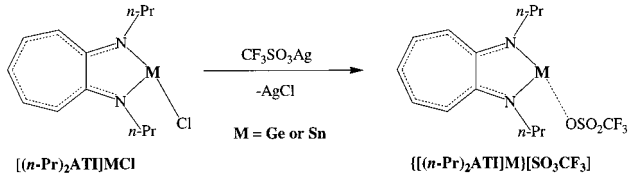

[(*n*-Pr)$_2$ATI]MCl {[(*n*-Pr)$_2$ATI]M}[SO_3CF_3]

the corresponding tin adducts feature longer M−N and M−Cl bonds and smaller N−M−N angles. This is expected on the basis of the relatively larger atomic radius of tin. These chloro adducts may also be compared to [(Mes)$_2$DAP]MCl[26] and [(Dipp)$_2$DAP]MCl.[27] Both aminotroponiminato (ATI) and diazapentadienyl (DAP) (also known as β-diketiminato) systems are monoanionic, bidentate, nitrogen based ligands, and feature conjugated ligand backbones. Structures of these Ge(II) and Sn(II) ATI derivatives show planar C_7N_2M rings whereas the related DAP adducts show nonplanar C_3N_2M rings in which the metal atom usually resides out of plane. A comparison of M−N distances shows that, for a given M, they are somewhat similar between the ATI and DAP systems (Table 2). However, N−M−N angles are notably different (e.g., N−Ge−N angle 81.4(2)° in [(*n*-Pr)$_2$ATI]GeCl and 90.44(9)° in [(Mes)$_2$DAP]GeCl). This is due to the size difference of the metallacycles in which aminotroponiminates form five-membered ring systems whereas diazapentadienyl adducts feature six-membered metallacycles.[11]

Syntheses of the cationic Ge(II) and Sn(II) compounds {[(*n*-Pr)$_2$ATI]Ge}[SO_3CF_3] and {[(*n*-Pr)$_2$ATI]Sn}[SO_3CF_3] were achieved by reacting [(*n*-Pr)$_2$ATI]GeCl and [(*n*-Pr)$_2$ATI]-SnCl with CF_3SO_3Ag in CH_2Cl_2 (Scheme 2). These silver salt metathesis reactions are quite rapid, as evident from the immediate precipitation of AgCl. The cationic species are much less soluble in hydrocarbon solvents than the corresponding chloro compounds. The Ge(II) species {[(*n*-Pr)$_2$-ATI]Ge}[SO_3CF_3] is soluble in warm toluene, while the Sn(II) species {[(*n*-Pr)$_2$ATI]Sn}[SO_3CF_3] exhibits poor solubility even in hot toluene and only moderate solubility in CH_2Cl_2. The melting points of these compounds are significantly higher than those of their chloro analogues. The ^{1}H NMR resonances of the ring protons of {[(*n*-Pr)$_2$ATI]Ge}-[SO_3CF_3] show a significant downfield shift relative to those of [(*n*-Pr)$_2$ATI]GeCl. A similar trend, but to a lesser degree,

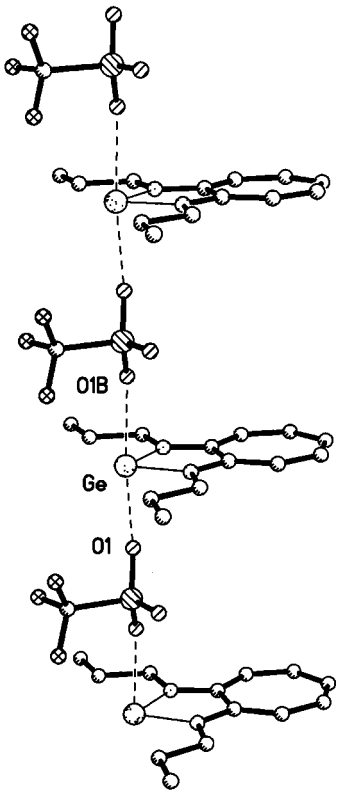

Figure 3. Representation of the X-ray crystal structure of {[(*n*-Pr)$_2$ATI]-Ge}[CF_3SO_3] showing weak Ge···O interactions (hydrogen atoms not shown). Selected bond lengths (Å) and angles (deg) are as follows: Ge−N(1), 1.930(5); Ge−N(9), 1.918(5); N(1)−C(2), 1.353(8); N(1)−C(10), 1.453(7); N(9)−C(8), 1.356(7); N(9)−C(13), 1.476(7); S−O(2), 1.405(5); S−O(1), 1.441(3); S−O(1)A, 1.441(3); Ge···O1, 2.483; Ge···O1B, 2.483; N(9)−Ge−N(1), 81.4(2); C(2)−N(1)−C(10), 120.9(5); C(2)−N(1)−Ge, 116.5(4); C(10)−N(1)−Ge, 122.6(4); C(8)−N(9)−C(13), 119.9(5); C(8)−N(9)−Ge, 116.4(4); C(13)−N(9)−Ge, 123.8(4); O···Ge···O1B, 192.2.

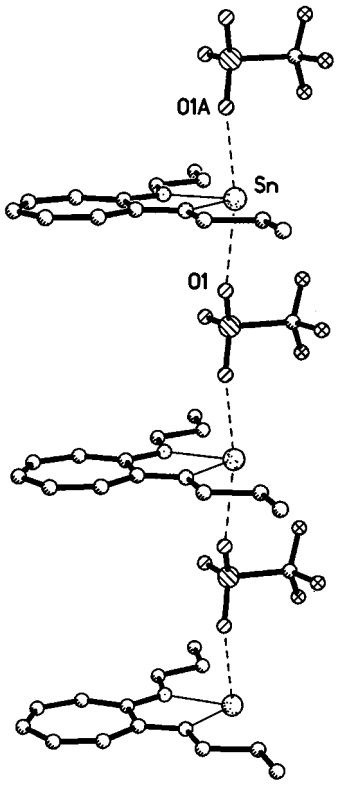

Figure 4. Representation of the X-ray crystal structure of {[(*n*-Pr)$_2$ATI]-Sn}[CF_3SO_3] showing weak Sn···O interactions (hydrogen atoms not shown). Selected bond lengths (Å) and angles (deg) are as follows: Sn−N(9), 2.125(5); Sn−N(1), 2.131(5); Sn···O(1), 2.513(4); Sn···O(1)A, 2.513(4); S−O(2), 1.403(5); S−O(1), 1.434(4); S−O(1)B, 1.434(4); N(1)−C(2), 1.341(9); N(1)−C(10), 1.468(8); N(9)−C(8), 1.342(8); N(9)−C(13), 1.468(8); N(9)−Sn−N(1), 75.03(19); N(9)−Sn−O(1), 83.06(8); N(1)−Sn−O(1), 86.45(10); N(9)−Sn−O(1)A, 83.06(8); N(1)−Sn−O(1)A, 86.45(10); O(1)···Sn···O(1)A, 194.36(16); O(2)−S−O(1), 116.4(2); O(2)−S−O(1)B, 116.4(2); O(1)−S−O(1)B, 111.5(3); C(2)−N(1)−C(10), 120.0(5); C(2)−N(1)−Sn, 118.0(4); C(10)−N(1)−Sn, 122.0(4); C(8)−N(9)−C(13), 119.3(5); C(8)−N(9)−Sn, 118.4(4); C(13)−N(9)−Sn, 122.3(4).

is observed for {[(*n*-Pr)$_2$ATI]Sn}[SO_3CF_3] when compared to its chloro analogue. The observed downfield shift of the ring protons in the cations may be indicative of the increased positive charge on the ATI ligand backbone. Indeed, the ability of the aminotroponiminate ligand backbone to stabilize the positive charge of the cations may help explain the usefulness of these ligands in stabilizing cationic, two-coordinate Ge(II) and Sn(II) species such as {[(*i*-Pr)$_2$ATI]-Ge}$^+$ and {[(*i*-Pr)$_2$ATI]Sn}$^+$.[12,13]

The X-ray crystal structures of {[(*n*-Pr)$_2$ATI]Ge}[SO_3CF_3] and {[(*n*-Pr)$_2$ATI]Sn}[SO_3CF_3] are shown in Figures 3 and 4, respectively. Overall, these two trifluoromethanesulfonate compounds show similar solid-state structures with $CF_3SO_3^-$ groups bridging {[(*n*-Pr)$_2$ATI]M}$^+$ moieties in a very symmetrical fashion. The Ge and Sn centers feature a pseudo-trigonal bipyramidal geometry with the metal lone pair occupying one of the equatorial sites and the bridging oxygens occupying axial positions. The O−Ge−O and O−Sn−O angles are 192.2° and 194.4°, respectively. Both {[(*n*-Pr)$_2$ATI]Ge}[SO_3CF_3] and {[(*n*-Pr)$_2$ATI]Sn}[SO_3CF_3] have planar C_5N_2M ring systems. They reside on a crystallographically imposed mirror plane.

The Ge−O distance for {[(*n*-Pr)$_2$ATI]Ge}[SO_3CF_3] is 2.483 Å, while the Ge−O distance for the previously reported {[(*i*-Pr)$_2$ATI]Ge}[SO_3CF_3] is 2.255(2) Å.[12] Therefore, changing the substituent on the nitrogen atoms of the aminotroponiminate ligand system from isopropyl to *n*-propyl increases the cation−anion separation by about 0.23 Å. This long Ge−O distance for {[(*n*-Pr)$_2$ATI]Ge}[SO_3CF_3] suggests only a very weak interaction between the germanium center and the trifluoromethanesulfonate anion (compare also to the sum of the covalent radii of Ge and O = 1.95 Å).[30] The Sn−O distance of 2.513(4) Å for {[(*i*-Pr)$_2$ATI]Sn}[SO_3CF_3] is also long and may be compared to the Sn−O distances for other tin(II) trifluoromethanesulfonates, such as [HB(3,5-$(CF_3)_2$-Pz)$_3$]Sn(OSO_2CF_3) (2.507(3) Å),[31] [Sn(η^2-CF_3SO_3){N(Si-$Me_3)_2$}]$_2$ (2.291(4) Å and 2.489(4) Å),[32] and [(Dipp)$_2$DAP]-Sn(OSO_2CF_3) (2.254(2) Å).[27] The structural parameters listed in Table 2 reveal that, despite the difference in the anion and despite the solid state arrangement of the trifluoromethanesulfonate compounds and the corresponding chloro derivatives (e.g., polymeric vs monomeric), there is some similarity in the bond lengths and angles (see, for example, Ge−N and N−Ge−N).

(30) Winter, M. WebElements. http://www.webelements.com (accessed 2001).
(31) Dias, H. V. R.; Jin, W. *Inorg. Chem.* **2000**, *39*, 815−819.
(32) Hitchcock, P. B.; Lappert, M. F.; Lawless, G. A.; de Lima, G. M.; Pierssens, L. J. M. *J. Organomet. Chem.* **2000**, *601*, 142−146.

Scheme 3. Attempted silver salt metathesis using $[HB(3,5\text{-}(CF_3)_2Pz)_3]Ag(\eta^2\text{-toluene})$.

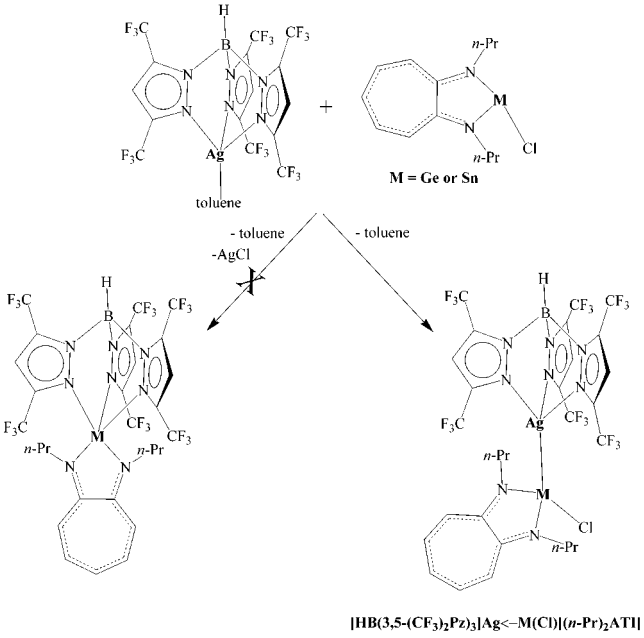

Compounds of the type LMX′, where X′ is a group other than a halide and M = Ge(II) or Sn(II), are not explored widely.[27] There is also interest in compounds with trifluoromethanesulfonate ligands, as they show diverse coordination modes (e.g., from ionic to mono-, bi-, or tridentate, terminal or bridging).[32] $\{[(n\text{-}Pr)_2ATI]Ge\}[SO_3CF_3]$ and $\{[(n\text{-}Pr)_2ATI]Sn\}[SO_3CF_3]$ are two new additions to these families.

Interestingly, when $[(n\text{-}Pr)_2ATI]GeCl$ and $[(n\text{-}Pr)_2ATI]SnCl$ were mixed with $[HB(3,5\text{-}(CF_3)_2Pz)_3]Ag(\eta^2\text{-toluene})$ in CH_2Cl_2, metathesis did not occur (Scheme 3). Instead, the 1:1 adducts $[HB(3,5\text{-}(CF_3)_2Pz)_3]Ag\leftarrow Ge(Cl)[(n\text{-}Pr)_2ATI]$ and $[HB(3,5\text{-}(CF_3)_2Pz)_3]Ag\leftarrow Sn(Cl)[(n\text{-}Pr)_2ATI]$ were formed in very high yields. These compounds did not precipitate AgCl even after several days in toluene or CH_2Cl_2. They exhibit excellent solubility in hydrocarbon solvents such as hexane and toluene. The ^1H NMR resonances of the ATI ring protons of $[HB(3,5\text{-}(CF_3)_2Pz)_3]Ag\leftarrow Ge(Cl)[(n\text{-}Pr)_2ATI]$ show a downfield shift relative to those of $[(n\text{-}Pr)_2ATI]GeCl$, although the shift is not as large as that noted for the cationic species $\{[(n\text{-}Pr)_2ATI]Ge\}[SO_3CF_3]$. The tin adduct $[HB(3,5\text{-}(CF_3)_2Pz)_3]Ag\leftarrow Sn(Cl)[(n\text{-}Pr)_2ATI]$ also shows this downfield shift in the ^1H NMR resonances of the ring protons when compared to the adduct free compound $[(n\text{-}Pr)_2ATI]SnCl$.

The NMR (^1H, ^{13}C, ^{19}F) spectra of $[HB(3,5\text{-}(CF_3)_2Pz)_3]Ag\leftarrow Ge(Cl)[(n\text{-}Pr)_2ATI]$ and $[HB(3,5\text{-}(CF_3)_2Pz)_3]Ag\leftarrow Sn(Cl)[(n\text{-}Pr)_2ATI]$ display resonances for three equivalent pyrazolyl rings. Chemical shift values corresponding to the tris(pyrazolyl)borate moiety are very similar to those observed for various $[HB(3,5\text{-}(CF_3)_2Pz)_3]^-$ adducts.[8,17−19,31,33−39] For example, ^{19}F NMR spectra show two signals, as expected for the CF_3 groups on the 3- and 5-positions of the pyrazole ring. The signal that corresponds to the trifluoromethyl groups on the pyrazole ring 5-position appears as a doublet. This is believed to be due to long-range coupling to the hydrogen atom on boron.[17] Interestingly, the ^{19}F NMR spectrum of $[HB(3,5\text{-}(CF_3)_2Pz)_3]Ag\leftarrow Ge(Cl)[(n\text{-}Pr)_2ATI]$ also shows long-range coupling between Ag and F atoms.[17,19]

The ^{119}Sn NMR spectroscopic data of $[HB(3,5\text{-}(CF_3)_2Pz)_3]Ag\leftarrow Sn(Cl)[(n\text{-}Pr)_2ATI]$ clearly suggest a strong interaction between the silver ion and the tin center in solution. The spectrum shows a broad doublet centered at 117 ppm with $^1J(^{119}Sn-^{109/107}Ag) = 5234$ Hz. There are only two other structurally characterized compounds in the literature to our knowledge in which one-bond $^{109/107}Ag-^{119}Sn$ coupling constants have been reported. They are $[HB(3,5\text{-}(CF_3)_2Pz)_3]AgSn(N_3)[(n\text{-}Pr)_2ATI]$ and $[(thf)Ag(\mu\text{-}SCN)Sn\{CH(SiMe_3)_2\}_2]_2$ and show broad signals at 90 ppm ($^1J(^{119}Sn-^{109/107}Ag) = 4866$ Hz)[40] and 250 ppm ($^1J(^{119}Sn-^{109}Ag) = 4632$, $^1J(^{119}Sn-^{107}Ag) = 4063$ Hz)[41] in their ^{119}Sn NMR spectra, respectively. The silver-free $[(n\text{-}Pr)_2ATI]SnCl$ displays a broad singlet at a higher frequency (−84 ppm).

The X-ray crystal structures of $[HB(3,5\text{-}(CF_3)_2Pz)_3]Ag\leftarrow Ge(Cl)[(n\text{-}Pr)_2ATI]$ and $[HB(3,5\text{-}(CF_3)_2Pz)_3]Ag\leftarrow Sn(Cl)[(n\text{-}Pr)_2ATI]$ are illustrated in Figures 5 and 6, respectively. They feature unsupported Ag−Ge and Ag−Sn bonds. The Ag−Ge bond distance of $[HB(3,5\text{-}(CF_3)_2Pz)_3]Ag\leftarrow Ge(Cl)[(n\text{-}Pr)_2ATI]$ may be compared to the Ag−Ge bond distances of 2.4113(8) Å for $[HB(3,5\text{-}(CF_3)_2Pz)_3]Ag\leftarrow Ge(CF_3SO_3)[(Me)_2ATI]$[8] and 2.4146(7) Å for $[HB(3,5\text{-}(CF_3)_2Pz)_3]AgGe(N_3)[(n\text{-}Pr)_2ATI]$.[40] The Ag−Sn bond distance of 2.5863(6) Å for $[HB(3,5\text{-}(CF_3)_2Pz)_3]Ag\leftarrow Sn(Cl)[(n\text{-}Pr)_2ATI]$ is the shortest among the structurally characterized Sn−Ag adducts reported to date. They include $[MeSi\{Si(Me)_2N(p\text{-}Tol)\}_3SnAg]_2$ (2.6567(7) Å),[42] $[(thf)Ag(\mu\text{-}SCN)Sn\{CH(SiMe_3)_2\}_2]_2$ (2.598(1) Å),[41] and $[HB(3,5\text{-}(CF_3)_2Pz)_3]AgSn(N_3)[(n\text{-}Pr)_2ATI]$ (2.5943(6) Å).[40]

As observed in Table 3, the silver adduct compounds $[HB(3,5\text{-}(CF_3)_2Pz)_3]Ag\leftarrow M(Cl)[(n\text{-}Pr)_2ATI]$ (where M = Ge or Sn) show shorter $M-N_{ring}$ bonds, larger $N_{ring}-M-N_{ring}$ angles, and shorter M−Cl bonds than their precursor compounds $[(n\text{-}Pr)_2ATI]MCl$ (M = Ge or Sn). This is probably a result of an increased s-character of the $M-N_{ring}$ and M−Cl bonds due to silver ion coordination to the metal center.

It is also noteworthy that Sn(II)−Ag(I) systems are of interest because of the importance of $SnCl_2$ in photography applications as a reduction sensitizer for silver halide emulsions.[42]

To investigate the role of the halide in silver salt metathesis reactions, $[(n\text{-}Pr)_2ATI]SnI$ was prepared by treating SnI_2 with

(33) Dias, H. V. R.; Lu, H.-L. *Inorg. Chem.* **1995**, *34*, 5380−5382.
(34) Dias, H. V. R.; Jin, W. *J. Am. Chem. Soc.* **1995**, *117*, 11381−11382.
(35) Dias, H. V. R.; Jin, W. *Inorg. Chem.* **1996**, *35*, 267−268.
(36) Dias, H. V. R.; Lu, H.-L.; Gorden, J. D.; Jin, W. *Inorg. Chem.* **1996**, *35*, 2149−2151.
(37) Dias, H. V. R.; Kim, H.-J.; Lu, H.-L.; Rajeshwar, K.; Tacconi, N. R.; Derecskei-Kovacs, A.; Marynick, D. S. *Organometallics* **1996**, *15*, 2994−3003.
(38) Dias, H. V. R.; Polach, S. A.; Goh, S.-K.; Archibong, E. F.; Marynick, D. S. *Inorg. Chem.* **2000**, *39*, 3894−3901.
(39) Dias, H. V. R.; Jin, W. *Inorg. Chem.* **1996**, *35*, 3687−3694.
(40) Dias, H. V. R.; Ayers, A. *Polyhedron* **2002**, *21*, 611−618.
(41) Hitchcock, P. B.; Lappert, M. F.; Pierssens, L. J.-M. *Organometallics* **1998**, *17*, 2686−2688.

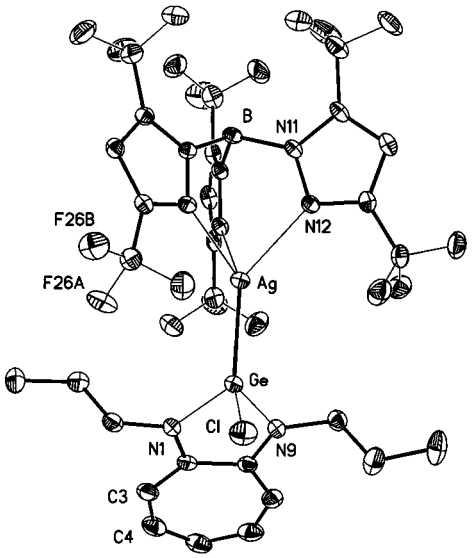

Figure 5. Representation of the X-ray crystal structure of [HB(3,5-$(CF_3)_2$-Pz)$_3$]Ag←Ge(Cl)[(*n*-Pr)$_2$ATI] (hydrogen atoms not shown). Selected bond lengths (Å) and angles (deg) are as follows: Ag−N(22), 2.355(3); Ag−N(32), 2.394(3); Ag−N(12), 2.399(3); Ag−Ge, 2.4142(6); Ge−N(9), 1.894(3); Ge−N(1), 1.898(3); Ge−Cl, 2.2270(11); N(1)−C(2), 1.348(5); N(1)−C(10), 1.462(5); N(9)−C(8), 1.343(5); N(9)−C(13′), 1.469(5); N(11)−B, 1.547(5); N(21)−B, 1.557(5); N(31)−B, 1.559(5); N(22)−Ag−N(32), 81.94(9); N(22)−Ag−N(12), 78.70(9); N(32)−Ag−N(12), 75.66(9); N(22)−Ag−Ge, 131.65(7); N(32)−Ag−Ge, 126.63(7); N(12)−Ag−Ge, 140.02(7); N(9)−Ge−N(1), 82.94(13); N(9)−Ge−Cl, 102.43(10); N(1)−Ge−Cl, 98.55(10); N(9)−Ge−Ag, 121.18(9); N(1)−Ge−Ag, 124.29(9); Cl−Ge−Ag, 119.77(3); C(2)−N(1)−C(10), 123.8(3); C(2)−N(1)−Ge, 115.3(2); C(10)−N(1)−Ge, 120.7(2); C(8)−N(9)−C(13′), 123.3(3); C(8)−N(9)−Ge, 116.1(2); C(13′)−N(9)−Ge, 120.6(2); N(11)−B−N(21), 109.8(3); N(11)−B−N(31), 109.2(3); N(21)−B−N(31), 110.2(3).

[(*n*-Pr)$_2$ATI]Li in a 1:1 molar ratio in Et_2O. ^{1}H and ^{13}C NMR data for [(*n*-Pr)$_2$ATI]SnI show very similar chemical shift values to the values observed for [(*n*-Pr)$_2$ATI]SnCl. The ^{119}Sn NMR, however, reveals a significant downfield shift in the ^{119}Sn signal (δ 19) when compared to the ^{119}Sn signal for [(*n*-Pr)$_2$ATI]SnCl (δ −84). The X-ray crystal structure of [(*n*-Pr)$_2$ATI]SnI is shown in Figure 7. The asymmetric unit contains two chemically similar but crystallographically different molecules. As seen in Table 2, key structural parameters for [(*n*-Pr)$_2$ATI]SnI are almost identical to the corresponding values for [(*n*-Pr)$_2$ATI]SnCl with the notable exception of Sn−halide bond length.

When [(*n*-Pr)$_2$ATI]SnI was mixed with [HB(3,5-$(CF_3)_2$-Pz)$_3$]Ag(η^2-toluene) in CH_2Cl_2, the 1:1 adduct [HB(3,5-$(CF_3)_2$Pz)$_3$]Ag←Sn(I)[(*n*-Pr)$_2$ATI] was formed in high yield. Even though [(*n*-Pr)$_2$ATI]SnI has a longer tin−halide bond length than [(*n*-Pr)$_2$ATI]SnCl by approximately 0.4 Å and a weaker tin−halide bond (e.g., Sn−Cl and Sn−I bond enthalpies are 414 ± 17 and 234 ± 42 kJ mol^{-1}, respectively),[30] no metathesis was observed even after several days. The ^{1}H NMR resonances of the ATI ring protons show a downfield shift when compared to the resonances for [(*n*-Pr)$_2$ATI]SnI. This trend was also noted for the chloro analogue. In addition, the ^{119}Sn NMR for [HB(3,5-$(CF_3)_2$-Pz)$_3$]Ag←Sn(I)[(*n*-Pr)$_2$ATI] reveals a downfield shift in the

(42) Findeis, B.; Gade, L. H.; Scowen, I. J.; McPartlin, M. *Inorg. Chem.* **1997**, *36*, 960−961.

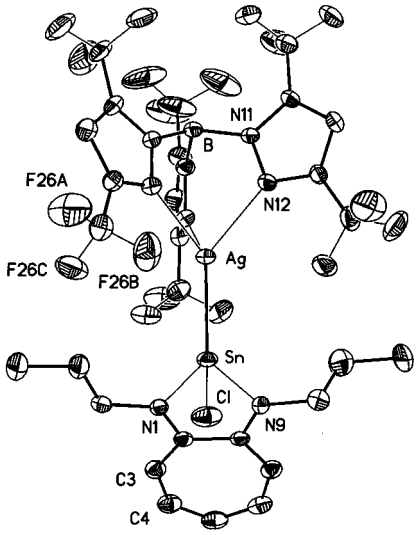

Figure 6. Representation of the X-ray crystal structure of [HB(3,5-$(CF_3)_2$-Pz)$_3$]Ag←Sn(Cl)[(*n*-Pr)$_2$ATI] (hydrogen atoms not shown). Selected bond lengths (Å) and angles (deg) are as follows: Ag−N(22), 2.353(4); Ag−N(12), 2.396(4); Ag−N(32), 2.401(5); Ag−Sn, 2.5863(6); Sn−N(9), 2.090(5); Sn−N(1), 2.098(4); Sn−Cl, 2.4082(18); N(1)−C(2), 1.337(7); N(1)−C(10), 1.465(7); N(9)−C(8), 1.346(7); N(9)−C(13′), 1.482(8); N(11)−B, 1.556(8); N(21)−B, 1.548(9); N(31)−B, 1.552(9); N(22)−Ag−N(12), 77.29(16); N(22)−Ag−N(32), 82.12(16); N(12)−Ag−N(32), 80.54(16); N(22)−Ag−Sn, 136.05(12); N(12)−Ag−Sn, 139.14(11); N(32)−Ag−Sn, 120.14(11); N(9)−Sn−N(1), 76.59(18); N(9)−Sn−Cl, 95.89(15); N(1)−Sn−Cl, 97.64(13); N(9)−Sn−Ag, 123.89(14); N(1)−Sn−Ag, 123.55(12); Cl−Sn−Ag, 126.33(4); C(2)−N(1)−C(10), 121.2(4); C(2)−N(1)−Sn, 116.5(3); C(10)−N(1)−Sn, 122.3(3); C(8)−N(9)−C(13′), 124.3(5); C(8)−N(9)−Sn, 117.2(4); C(13′)−N(9)−Sn, 118.4(5); N(21)−B−N(31), 111.5(5); N(21)−B−N(11), 109.3(5); N(31)−B−N(11), 110.0(5).

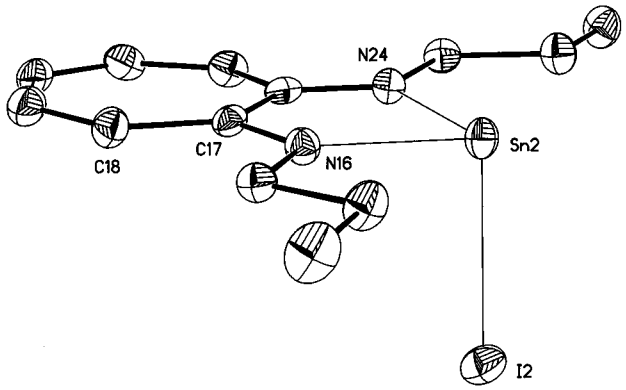

Figure 7. Representation of the X-ray crystal structure of [(*n*-Pr)$_2$ATI]-SnI (hydrogen atoms and the second molecule in the asymmetric unit not shown). Selected bond lengths (Å) and angles (deg) are as follows. *Molecule 1*: Sn(1)−N(1), 2.145(6); Sn(1)−N(9), 2.154(5); Sn(1)−I(1), 2.8837(7); N(1)−C(2), 1.318(8); N(1)−C(10), 1.595(12); N(9)−C(8), 1.330(8); N(9)−C(13), 1.455(7); N(1)−Sn(1)−N(9), 74.19(19); N(1)−Sn(1)−I(1), 92.44(19); N(9)−Sn(1)−I(1), 92.23(13); C(2)−N(1)−C(10), 123.3(6); C(2)−N(1)−Sn(1), 118.6(4); C(10)−N(1)−Sn(1), 117.3(4); C(8)−N(9)−C(13), 120.9(5); C(8)−N(9)−Sn(1), 117.8(4); C(13)−N(9)−Sn(1), 121.3(4). *Molecule 2*: Sn(2)−N(16), 2.148(5); Sn(2)−N(24), 2.151(4); Sn(2)−I(2), 2.9310(7); N(16)−C(17), 1.338(7); N(16)−C(25), 1.457(7); N(24)−C(23), 1.320(7); N(24)−C(28), 1.470(7); N(16)−Sn(2)−N(24), 74.23(17); N(16)−Sn(2)−I(2), 94.43(13); N(24)−Sn(2)−I(2), 91.71(12); C(17)−N(16)−C(25), 119.7(5); C(17)−N(16)−Sn(2), 117.9(4); C(25)−N(16)−Sn(2), 122.4(4); C(23)−N(24)−C(28), 120.4(5); C(23)−N(24)−Sn(2), 118.4(4); C(28)−N(24)−Sn(2), 121.2(4).

^{119}Sn signal (δ 111) when compared to that of [(*n*-Pr)$_2$ATI]-SnI (δ 19). The ^{119}Sn signal for [HB(3,5-$(CF_3)_2$Pz)$_3$]Ag←Sn(I)[(*n*-Pr)$_2$ATI] occurs at a very close chemical shift value

Table 3. Selected Bond Lengths (Å) and Angles (deg) and ^{119}Sn NMR Spectroscopic Data (ppm) for [(*n*-Pr)$_2$ATI]MX and [HB(3,5-(CF$_3$)$_2$Pz)$_3$]Ag←M(X)[(*n*-Pr)$_2$ATI] (M = Ge or Sn, X = Cl or I; N_{ring} Refers to Values Involving the ATI Ring)

	[(*n*-Pr)$_2$ATI]GeCl	[HB(3,5-(CF$_3$)$_2$Pz)$_3$]Ag← Ge(Cl)[(*n*-Pr)$_2$ATI]
Ge−N_{ring}	1.936(2)	1.896(3)
Ge−Cl	2.3776(8)	2.2270(11)
Ge−Ag		2.4142(6)
N_{ring}−Ge−N_{ring}	80.24(8)	82.94(13)
	[(*n*-Pr)$_2$ATI]SnCl	[HB(3,5-(CF$_3$)$_2$Pz)$_3$]Ag← Sn(Cl)[(*n*-Pr)$_2$ATI]
Sn−N_{ring}	2.154(3)	2.094(4)
Sn−Cl	2.504(1)	2.4082(18)
Sn−Ag		2.5863(6)
N_{ring}−Sn−N_{ring}	73.9(1)	76.59(18)
^{119}Sn NMR	−84	117
	[(*n*-Pr)$_2$ATI]SnI	[HB(3,5-(CF$_3$)$_2$Pz)$_3$]Ag← Sn(I)[(*n*-Pr)$_2$ATI]
Sn−N_{ring}	2.149(5)	2.092(6)
Sn−I	2.9073(7)	2.8073(10)
Sn−Ag		2.5880(10)
N_{ring}−Sn−N_{ring}	74.2(1)	76.1(2)
^{119}Sn NMR	19	111

to that for [HB(3,5-(CF$_3$)$_2$Pz)$_3$]Ag←Sn(Cl)[(*n*-Pr)$_2$ATI] (δ 117). However, the $^1J(^{119}\text{Sn}-^{109/107}\text{Ag})$ of 4359 Hz for the iodo compound is markedly less than the $^1J(^{119}\text{Sn}-^{109/107}\text{Ag})$ of 5234 Hz for the chloro compound. This difference may be a result of steric effects, that is, the larger iodo group affecting the Ag−Sn separation in the *solution* structures. However, as we see later, *solid-state* data show essentially identical Ag−Sn and Sn−N_{ring} bond distances for the two analogues.

The X-ray crystal structure for [HB(3,5-(CF$_3$)$_2$Pz)$_3$]Ag←Sn(I)[(*n*-Pr)$_2$ATI] is shown in Figure 8 and reveals a silver−tin bond. No Ag−I bonding is observed for this compound, as proposed for CpFe(CO)$_2$I→Ag(B$_{11}$CH$_{12}$)[1] and observed structurally for [CpMo(CO)$_3$I→Ag(CB$_{11}$H$_{12}$)]$_2$.[5,6] Apparently, the lone pair on tin is a much more attractive Lewis base to silver than any lone pairs on the iodo group. The Sn−Ag bond length of 2.5880(10) Å is basically identical to the Sn−Ag bond length of 2.5863(6) Å observed for [HB(3,5-(CF$_3$)$_2$Pz)$_3$]Ag←Sn(Cl)[(*n*-Pr)$_2$ATI]. In a manner similar to that for the chloro compounds, [HB(3,5-(CF$_3$)$_2$Pz)$_3$]Ag←Sn(I)[(*n*-Pr)$_2$ATI] shows a shortening of the Sn−I and Sn−N_{ring} bonds and a widening of the N_{ring}−Sn−N_{ring} angle when compared to the nonsilver adduct compound [(*n*-Pr)$_2$ATI]SnI (Table 3).

Summary and Conclusion

This work demonstrates the key role that the anion of the silver salt plays in the silver salt metathesis process. We have also investigated the effect of the halide source (Ge vs Sn) and the halide ion (Cl vs I). In this work, instant metathesis occurs with trifluoromethanesulfonate as the anion but not with hydrotris(3,5-bis(trifluoromethyl)pyrazolyl)borate as the anion. Furthermore, the presence of a lone pair on the metal center of the halide source provides a route to interesting adduct compounds featuring unsupported metal−silver bonds

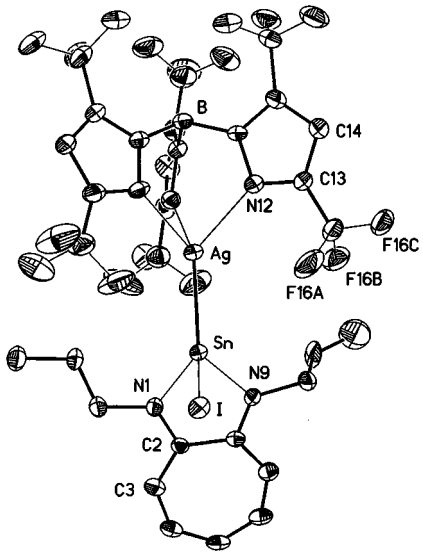

Figure 8. Representation of the X-ray crystal structure of [HB(3,5-(CF$_3$)$_2$Pz)$_3$]Ag←Sn(I)[(*n*-Pr)$_2$ATI] (hydrogen atoms not shown). Selected bond lengths (Å) and angles (deg) are as follows: Ag−N(12), 2.350(7); Ag−N(32), 2.357(7); Ag−N(22), 2.394(7); Ag−Sn, 2.5880(10); Sn−N(9), 2.089(6); Sn−N(1), 2.095(6); Sn−I, 2.8073(10); B−N(31), 1.544(12); B−N(21), 1.548(13); B−N(11), 1.554(12); N(1)−C(2), 1.342(9); N(1)−C(10), 1.476(10); N(9)−C(8), 1.339(9); N(9)−C(13′), 1.482(10); N(12)−Ag−N(32), 82.5(2); N(12)−Ag−N(22), 78.6(2); N(32)−Ag−N(22), 80.3(2); N(12)−Ag−Sn, 133.62(17); N(32)−Ag−Sn, 129.57(17); N(22)−Ag−Sn, 132.09(18); N(9)−Sn−N(1), 76.1(2); N(9)−Sn−Ag, 127.69(18); N(1)−Sn−Ag, 131.35(18); N(9)−Sn−I, 97.57(17); N(1)−Sn−I, 96.00(18); Ag−Sn−I, 117.48(3); N(31)−B−N(21), 110.8(7); N(31)−B−N(11), 109.3(7); N(21)−B−N(11), 109.2(7).

if silver salt metathesis is inhibited. Although we do not have any direct evidence, this work suggests that the metathesis reactions between [(*n*-Pr)$_2$ATI]MX and AgSO$_3$CF$_3$ may proceed via a Ag−M bonded intermediate. The results presented here involving heavier main group 14 elements are somewhat akin to the metathesis chemistry of the transition metal adduct (PPh$_3$)$_2$(CO)IrCl.[10]

We should also note that silver salt metathesis reaction between the silver derivatives of [HB(3,5-(CF$_3$)$_2$Pz)$_3$]$^-$ and Au(CO)Cl,[34] (CO)$_5$MnBr,[37] InCl,[35] or GaI[31] proceeds smoothly, leading to silver halide precipitates. Thus, the halide source also plays an important role in the metathesis process. Overall, this study and the results from previous work suggest that both the halide source and the anion of the silver salt have important roles in the outcome of a silver salt metathesis reaction. The mechanism also appears to be diverse, as evident from isolable intermediates featuring Ag−halide[5,6,9] and Ag−M[1,8,10] bonds.

Acknowledgment. We thank The Robert A. Welch Foundation (Grant Y-1289) for support of this work. We also thank the National Science Foundation (Grant CHE-9601771) for providing funds to purchase the 500 MHz NMR spectrometer.

Supporting Information Available: X-ray crystallographic files in CIF format. This material is available free of charge via the Internet at http://pubs.acs.org.

IC0200747